

# On-chip stimulated Brillouin scattering

Ravi Pant,<sup>1,2,\*</sup> Christopher G. Poulton,<sup>2,3</sup> Duk-Yong Choi,<sup>2,4</sup>  
Hannah McFarlane,<sup>1,2</sup> Samuel Hile,<sup>1,2</sup> Enbang Li,<sup>1,2</sup> Luc Thevenaz,<sup>5</sup>  
Barry Luther-Davies,<sup>2,4</sup> Stephen J. Madden,<sup>2,4</sup> and Benjamin J. Eggleton<sup>1,2</sup>

<sup>1</sup>Institute of Photonics and Optical Sciences (IPOS), School of Physics, University of Sydney, NSW 2006, Australia

<sup>2</sup>Centre for Ultrahigh-bandwidth Devices for Optical Systems (CUDOS), Australia

<sup>3</sup>School of Mathematical Sciences, University of Technology Sydney, NSW 2007, Australia

<sup>4</sup>Laser Physics Centre, Australian National University, Canberra, ACT 0200, Australia

<sup>5</sup>Institute of Electrical Engineering, Ecole Polytechnique Fédérale de Lausanne, 1015 Lausanne, Switzerland

\*rpant@physics.usyd.edu.au

**Abstract:** We demonstrate on-chip stimulated Brillouin scattering (SBS) in an As<sub>2</sub>S<sub>3</sub> chalcogenide rib waveguide. SBS was characterized in a 7cm long waveguide with a cross-section 4μm x 850nm using the backscattered signal and pump-probe technique. The measured Brillouin shift and its full-width at half-maximum (FWHM) linewidth were ~7.7 GHz and 34 MHz, respectively. Probe vs. pump power measurements at the Brillouin shift were used to obtain the gain coefficient from an exponential fit. The Brillouin gain coefficient obtained was 0.715 x 10<sup>-9</sup> m/W. A probe gain of 16 dB was obtained for a CW pump power of ~300 mW.

©2011 Optical Society of America

**OCIS codes:** (190.0190) Nonlinear optics; (190.2640) Stimulated scattering, modulation, etc.; (190.4360) Nonlinear optics, devices.

---

## References and links

1. R. W. Boyd, *Nonlinear Optics* (Academic Press, 2003).
2. L. Thévenaz, "Slow and fast light in optical fibres," *Nat. Photonics* **2**(8), 474–481 (2008).
3. T. Schneider, K. Jamshidi, and S. Preussler, "Quasi-Light Storage: A Method for the Tunable Storage of Optical Packets With a Potential Delay-Bandwidth Product of Several Thousand Bit," *J. Lightwave Technol.* **28**(17), 2586–2592 (2010).
4. M. J. Lee, R. Pant, and M. A. Neifeld, "Improved slow-light delay performance of a broadband stimulated Brillouin scattering system using fiber Bragg gratings," *Appl. Opt.* **47**(34), 6404–6415 (2008).
5. R. Pant, M. D. Stenner, M. A. Neifeld, and D. J. Gauthier, "Optimal pump profile designs for broadband SBS slow-light systems," *Opt. Express* **16**(4), 2764–2777 (2008).
6. Z. Shi, R. Pant, Z. Zhu, M. D. Stenner, M. A. Neifeld, D. J. Gauthier, and R. W. Boyd, "Design of a tunable time-delay element using multiple gain lines for increased fractional delay with high data fidelity," *Opt. Lett.* **32**(14), 1986–1988 (2007).
7. K. Y. Song, K. S. Abedin, K. Hotate, M. González Herráez, and L. Thévenaz, "Highly efficient Brillouin slow and fast light using As<sub>2</sub>Se<sub>3</sub> chalcogenide fiber," *Opt. Express* **14**(13), 5860–5865 (2006).
8. L. F. Stokes, M. Chodorow, and H. J. Shaw, "All-fiber stimulated Brillouin ring laser with submilliwatt pump threshold," *Opt. Lett.* **7**(10), 509–511 (1982).
9. K. Y. Song, S. Chin, N. Primerov, and L. Thevenaz, "Time-Domain Distributed Fiber Sensor With 1 cm Spatial Resolution Based on Brillouin Dynamic Grating," *J. Lightwave Technol.* **28**(14), 2062–2067 (2010).
10. S. Chin, L. Thévenaz, J. Sancho, S. Sales, J. Capmany, P. Berger, J. Bourderionnet, and D. Dolfi, "Broadband true time delay for microwave signal processing, using slow light based on stimulated Brillouin scattering in optical fibers," *Opt. Express* **18**(21), 22599–22613 (2010).
11. B. Zhang, L. S. Yan, J. Y. Yang, I. Fazal, and A. E. Willner, "A single slow-light element for independent delay control and synchronization on multiple gb/s data channels," *IEEE Photon. Technol. Lett.* **19**(14), 1081–1083 (2007).
12. M. D. Pelusi, A. Fu, and B. J. Eggleton, "Multi-channel in-band OSNR monitoring using Stimulated Brillouin Scattering," *Opt. Express* **18**(9), 9435–9446 (2010).
13. P. T. Rakich, P. Davids, and Z. Wang, "Tailoring optical forces in waveguides through radiation pressure and electrostrictive forces," *Opt. Express* **18**(14), 14439–14453 (2010).
14. J. C. Beugnot, T. Sylvestre, D. Alasia, H. Maillotte, V. Laude, A. Monteville, L. Provino, N. Traynor, S. F. Mafang, and L. Thévenaz, "Complete experimental characterization of stimulated Brillouin scattering in photonic crystal fiber," *Opt. Express* **15**(23), 15517–15522 (2007).
15. P. Dainese, P. S. J. Russell, N. Joly, J. C. Knight, G. S. Wiederhecker, H. L. Fragnito, V. Laude, and A. Khelif, "Stimulated Brillouin scattering from multi-GHz-guided acoustic phonons in nanostructured photonic crystal fibre," *Nat. Phys.* **2**(6), 388–392 (2006).

16. B. J. Eggleton, B. Luther-Davies, and K. Richardson, "Chalcogenide Photonics," *Nat. Photonics* **5**(3), 141–148 (2011).
17. B. J. Eggleton, "Chalcogenide photonics: fabrication, devices and applications. Introduction," *Opt. Express* **18**(25), 26632–26634 (2010).
18. L. Landau, and E. Lifshitz, *Theory of Elasticity* (Pergamon Press, 1959).
19. T. Han, S. Madden, D. Bulla, and B. Luther-Davies, "Low loss Chalcogenide glass waveguides by thermal nano-imprint lithography," *Opt. Express* **18**(18), 19286–19291 (2010).

## 1. Introduction

Stimulated Brillouin Scattering (SBS), whereby light interacts coherently with acoustic phonons [1], is a powerful and flexible mechanism for controlling light. SBS has been exploited in optical fibers based on silica and other glasses to achieve tunable slow-light (SL) [2–7] as well as to enable a range of important technologies such as Brillouin lasers [8]; sensors [9]; SBS SL based true-time delay for RADARs [10]; all-optical signal processing [11] and monitoring [12]; opto-mechanical oscillators and tailored optical forces [13]. Recently SBS was characterized in photonic crystal fibers (PCFs) [14, 15] where the strong confinement of the optical and acoustic modes provides strong photon-phonon interaction for exploiting SBS. While there have been several detailed studies of SBS in optical fibers, the ability to harness SBS in integrated optical chips is key to the realization of many applications in modern photonics that involve light-sound and light-light interactions. However, the investigation of on-chip SBS, in which the effect is induced in an integrated optical structure, has been limited because most platforms commonly used in nonlinear optics either have very small SBS gain coefficient (as is the case for Silica) or have negligible SBS even though they have very high Kerr nonlinearity (e.g. for Silicon). Chalcogenide glass, on the other hand, has both large SBS gain coefficient and Kerr nonlinearity [7, 16, 17] and therefore is a potential platform for exploiting SBS at the chip scale. SBS has already been characterized in chalcogenide fibers where large SBS gain coefficient leads to excitation in short devices [7].

In this paper, we characterize SBS in a 7 cm long  $\text{As}_2\text{S}_3$  chip using the backscattered signal and pump-probe techniques. The backscattered signal is used to estimate the Brillouin shift. Pump-probe measurements were then conducted to estimate the gain profile and Brillouin gain coefficient. The measured Brillouin shift and linewidth were 7.7 GHz and 34 MHz, respectively, which are consistent with the measured shift ( $\sim 7.9$ GHz) and linewidth ( $\sim 31$ MHz) in  $\text{As}_2\text{S}_3$  optical fibers. A probe gain of 16 dB was obtained at a CW pump power of  $\sim 300$  mW.

Figure 1 shows the principle of chip-based SBS where the interaction of light at frequency  $\omega_p$  (solid) with a travelling acoustic wave of frequency  $\Omega$  generates a backscattered signal (dashed) at the downshifted frequency  $\omega_s = \omega_p - \Omega_B$ . A scanning electron microscope (SEM) image of a typical rib waveguide is also shown in Fig. 1.

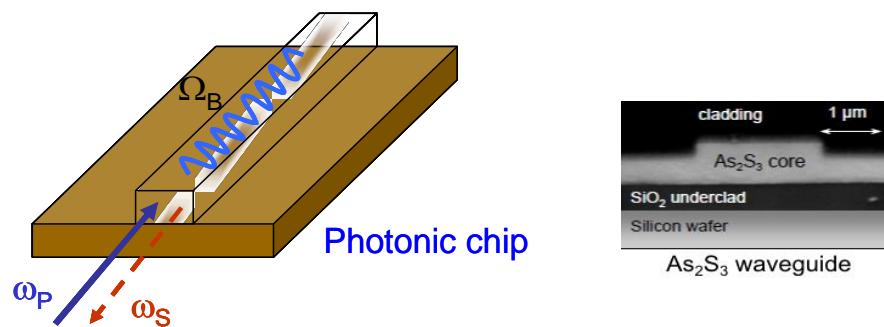


Fig. 1. Concept diagram of on-chip SBS showing the interaction of the pump signal (solid) of frequency ( $\omega_p$ ) with an acoustic wave of frequency ( $\Omega_B$ ) resulting in the generation of a backscattered signal at the downshifted frequency  $\omega_s = \omega_p - \Omega_B$  and SEM image of a typical rib chalcogenide waveguide.

## 2. Back reflection measurements

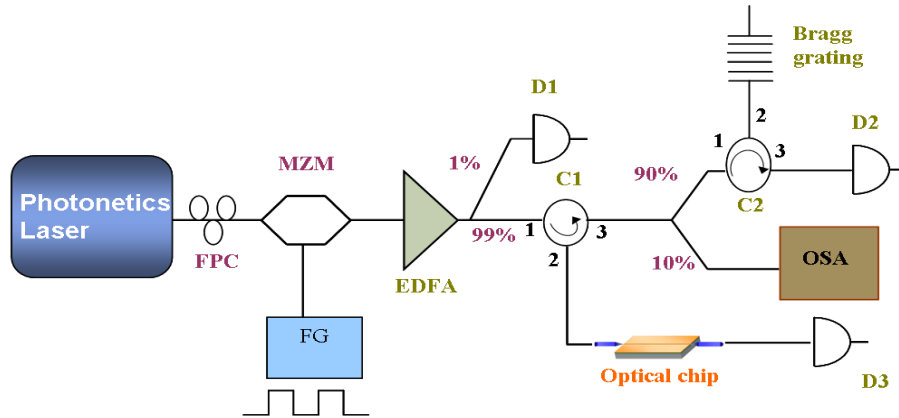


Fig. 2. Experimental set-up for investigating on-chip SBS using backscattered signal.

Figure 2 shows the experimental set-up for investigating SBS in our photonic chip. Light from a tunable Photonics laser at a pump wavelength ( $\lambda_p$ ) of  $\sim 1544.775$  nm was modulated using a 25 kHz pulse train from a function generator (FG) with a duty cycle of 1% to generate 400 ns pump pulses with their polarization controlled using a fiber polarization controller (FPC). These pulses were then amplified using a 1W Erbium doped fiber amplifier (EDFA) before they propagated to port 1 of the circulator 1 (C1). The input power was measured using detector 1 (D1) connected to 1% port of the 99/1 splitter. A lensed fiber at port 2 of the circulator was used to couple light into the waveguide. Back scattered light was collected at port 3 of the circulator and sent to a 90/10 splitter, where 90% of the light went to a Bragg grating via circulator 2 (C2) to measure the backscattered Stokes power on detector 2 (D2) and 10% to an optical spectrum analyzer (OSA). The pump power was collected at the output of the waveguide on detector 3 (D3). The waveguide has a cross-sectional area of  $4\mu\text{m} \times 850$  nm and was top clad with a 140 nm thick silica film, which acted as a protective layer. The total insertion loss for the waveguide was  $\sim 13.7$  dB, which included a loss of 4 dB at each facet.

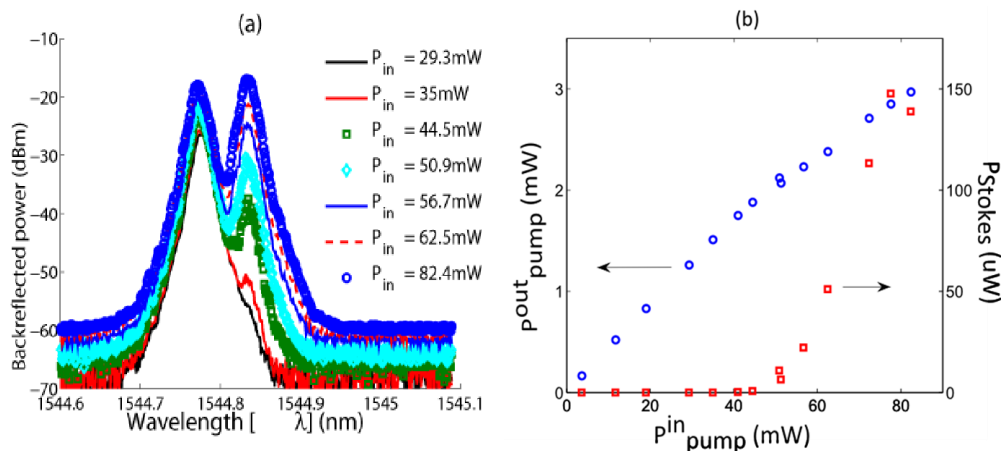


Fig. 3. Characterization of SBS using the backscattered signal showing (a) the spectra for the Rayleigh scattered pump and backscattered Stokes, for different input average pump powers (b) output pump power and filtered Stokes power as a function of the average input pump power.

Figures 3(a) and 3(b) show the measured backscattered spectra for different input average pump powers (before coupling to the waveguide), and the filtered Stokes and output pump power vs. input pump power respectively. The backscattered spectrum consists of Rayleigh scattered pump and backscattered Stokes signal. From Fig. 3(b) we note that the backscattered filtered Stokes signal power increases significantly at the critical input pump power of ~50mW, which corresponds to the coupled peak power of ~2.0W. In Fig. 3(b), we also observe that the output pump power increases linearly until the input reaches 50 mW after which the rate of increase of the output pump power reduces because of increased Stokes generation. From the backscattered spectrum, we estimate the Brillouin shift to be ~7.7 GHz.

### 3. Pump-probe measurements

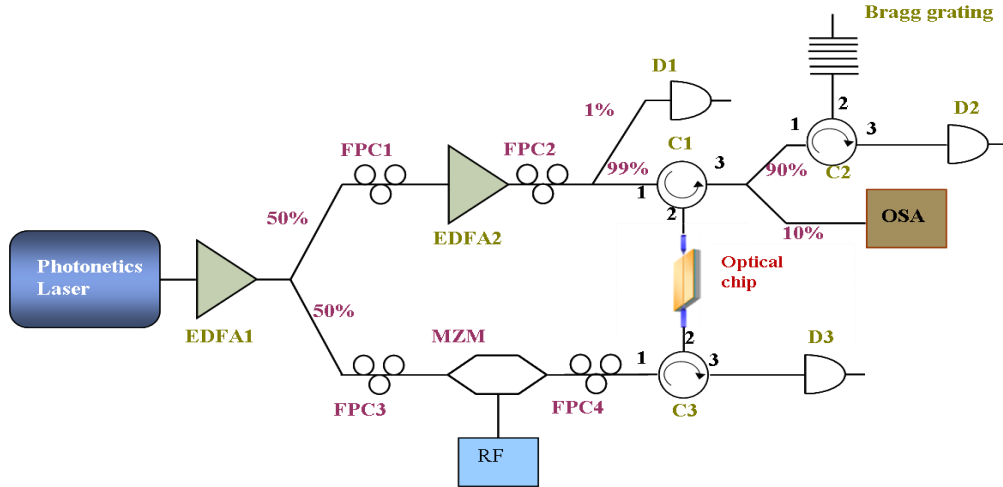


Fig. 4. Pump-probe set-up for measuring the SBS gain spectrum.

In order to measure the SBS gain spectrum, we performed pump-probe experiment using the set-up shown in Fig. 4. A 27dBm erbium doped fiber amplifier EDFA1 was used to amplify the laser power before it was coupled to a 50:50 splitter. A continuous wave (CW) pump and a counter-propagating, weak probe signal were used in the experiment. The pump was amplified using a 1 W EDFA. The probe was coupled to the waveguide via port 1 of circulator 3 (C3). The SBS gain spectrum was obtained using a fixed input pump power of 300 mW and measuring the probe power as the probe frequency was varied using a Mach-Zehnder modulator (MZM) driven by a radio frequency (RF) signal generator. The polarization of the pump and the probe signal were adjusted using FPCs 1-4 to maximize the gain.

Figures 5(a) shows the measured SBS gain spectrum and a Lorentzian fit. The measured Brillouin shift for the chip was ~7.7 GHz, which is consistent with the measured Brillouin shift in  $\text{As}_2\text{S}_3$  fiber, and the measured full-width at half-maximum (FWHM) line width was 34 MHz. We use the measured Brillouin shift and FWHM to calculate the gain coefficient for our photonic chip using the relation:

$$g_B = \eta \frac{4\pi n^8 P_{12}^2}{c \rho v_B \Delta v_B \lambda_p^3}, \quad (1)$$

where  $\eta$  is the overlap integral between the optical mode and acoustic mode induced density change;  $P_{12}$  is the longitudinal elasto-optic coefficient;  $c$  is the speed of light in vacuum;  $\rho$  is the material density;  $v_B$  is the Brillouin shift;  $\Delta v_B$  is the Brillouin linewidth and  $\lambda_p$  is the pump wavelength. Using the measured values of  $v_B$  and  $\Delta v_B$  in Eq. (1), we calculate  $g_B$  for our photonic chip to be  $0.74 \times 10^{-9}$  m/W. Here, we use the overlap integral  $\eta = 0.95$ , obtained

from the finite-element simulation,  $P_{12} = 0.24$ ,  $n = 2.37$  and  $\rho = 3200 \text{ Kg/m}^3$ . In order to obtain the value of  $\eta$ , both the optical and longitudinal acoustic modes were calculated for the waveguide. The longitudinal acoustic modes in waveguides were simulated by solving the equations of linear elasticity for a waveguide geometry. The imposition of translational symmetry in the waveguide direction, together with the application of appropriate boundary conditions (relating to continuity of the normal components of the stress tensor across material boundaries), leads to an eigenvalue problem for the frequency of the propagating mode. This problem was implemented and solved using a commercially available finite element solver (COMSOL). To confirm the predicted value of  $g_B$ , we measure the probe power at the Brillouin shift as the pump power was varied.

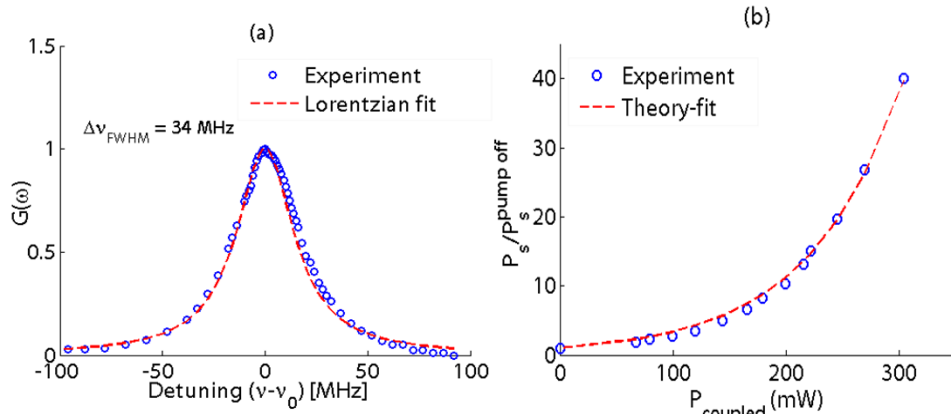


Fig. 5. Pump-probe measurements showing (a) the Brillouin gain spectrum obtained using the input pump power of 300 mW while the probe frequency is varied and (b) output probe power, at the Brillouin shift, normalized to the output probe power when the pump is off.

Figure 5(b) shows the measured probe vs. pump power at the Stokes frequency and the theoretical fit obtained using the following equation.

$$I_s(L) = I_s(0) \exp^{g_B \frac{P_{\text{pump}}}{A} L_{\text{eff}}}, \quad (2)$$

where  $I_s(L)$  and  $I_s(0)$  are the probe intensity respectively at the output and input of the device;  $g_B$  is the Brillouin gain coefficient;  $A$  is the effective mode area and  $L_{\text{eff}}$  is the effective length. In order to obtain  $g_B$ , we fit Eq. (2) to the measured probe vs. pump data using the effective optical mode area of  $2.3 \mu\text{m}^2$  and the effective length of 3.9 cm. From the fit, we obtain  $g_B$  of  $0.715 \times 10^{-9} \text{ m/W}$ , which is consistent with the value of  $0.74 \times 10^{-9} \text{ m/W}$  calculated using Eq. (1). From Fig. 5(b), we note that the probe experiences a gain factor of 43 ( $\sim 16 \text{ dB}$ ) for coupled pump power of 300 mW. We use the calculated gain coefficient to estimate the power required to achieve a probe gain of  $\sim 30 \text{ dB}$ , which is large enough for many applications. The required pump power is 577 mW. Currently the large propagation loss in our optical chip results in smaller effective length. The propagation loss can be further reduced to  $0.2 \text{ dB/cm}$  [19], which will double the effective length, halving the required pump power for the same gain.

Finally, we calculate the critical power ( $P_{cr}$ ) for the chip using the calculated gain coefficient in the following equation [7].

$$P_{cr} = 21 \frac{A_{\text{eff}}}{Kg_B L_{\text{eff}}}, \quad (3)$$

Where  $K$  is the parameter used to take into account polarization variation. Using the gain coefficient  $g_B = 0.715 \times 10^{-9}$  m/W and  $K = 1$  in Eq. (3), we obtain  $P_{th} \sim 1.73$  W, which is close to the critical peak power of  $\sim 2.0$  W obtained from the backscattering experiment.

In conclusion, we have demonstrated on-chip SBS using an optical chip built on  $As_2S_3$  platform. The measured Brillouin shift and linewidth were similar to that in  $As_2S_3$  optical fiber. The SBS gain coefficient obtained from the pump-probe measurement was consistent with the one obtained from Eq. (1). Exploiting SBS at chip-scale will enable better understanding of photon-phonon interaction for tailoring optical forces, fabricating compact, on-chip Brillouin lasers, slow-light devices, SBS slow-light based true-time delay for RADARs, and opto-mechanical oscillators.

### **Acknowledgements**

The support of the Australian Research Council (ARC) through its Discovery grant (DP1096838), Centre of Excellence scheme and ARC Federation Fellowship is gratefully acknowledged